Analysis of the deviation of the diffracted beams caused by acousto-optic tunable filter in multispectral imaging

Yu Yang (杨 瑀)[1*], Xuejun Sha (沙学军)[1], and Zhonghua Zhang (张中华)[2]

[1]*Department of Communication Engineering, Harbin Institute of Technology, Harbin 150001, China*

[2]*National Key Laboratory of Tunable Laser Technology, Harbin Institute of Technology, Harbin 150001, China*

[*]*Corresponding author: yangyu1118@hit.edu.cn*

Received December 31, 2010; accepted April 1, 2011; posted online May 31, 2011

The deviation caused by acousto-optic tunable filter (AOTF) diffraction in multispectral imaging is analyzed through derivation calculus of the deviation angle. The rotatory polarization of acousto-optic crystal is taken into account in this analysis. The relationships between the polar angle of the incident and the diffracted beams are acquired by using the momentum-matching condition. During the diffraction of the incident beams, far more deviations are induced.

OCIS codes: 110.0110, 080.0080.

doi: 10.3788/COL201109.081101.

Multispectral imaging systems have many applications in the fields of environmental and atmospheric monitoring[1], disease diagnosis[2], molecular biology[3], astronomy[4], and various other scientific investigations[5,6]. Multispectral imaging systems using an acousto-optic tunable filter (AOTF) have no moving parts and scan at very high rates (millisecond time scale). They can acquire the information parameters of spatial, spectral, polarization, and time coordinates of a scene. All the information parameters are available by controlling the electromagnetic wave medium and by tuning the frequency of a radio frepuency (RF) power that is supplied to a transducer mounted on the crystal[7]. In TeO_2 crystals, acoustic waves produce moving gratings that diffract optical incident beams. Acousto-optic diffraction processes are cumulative and built up continuously along the interaction region in the crystal.

Since TeO_2 crystals with high spatial resolution (typically 100 lines/mm) and large optical apertures are available, they can be applied for more spectral imaging applications[8]. Notwithstanding AOTF multispectral imaging system has attractive features, AOTFs have the problems of chromatic aberrations and monochromatic aberrations[9]. The dispersion of the crystal would cause wavelength dependence of the diffracted beam angle; the diffracted beam would shift with the scanning of the wavelength and spread with the band pass. The angle deviations of diffracted beams are a prime cause of aberrations, which can give rise to scene shifts and degrade the spatial resolution[10]. The monochromatic aberrations are a function of the collimation of the input beam, which can be minimized by placing the AOTF at a collimated pupil of the optical system, but they will still be present even for perfectly collimated light[11]. Many technologies were applied to the AOTF in Refs. [9,10] to minimize chromatic aberrations and monochromatic aberrations, but the rotatory property of TeO_2 was not taken into account in such papers. In this letter, we take into account the rotatory property of TeO_2 in analyzing the derivation of the deviation angle of the diffracted beams in AOTF multispectral imaging systems, and the derivate of the deviation angle and the polar angles of the incident and diffracted beams are calculated. According to the analysis, we advance a suitable value in designing the optical wedge at the output facet to reduce the adverse action of dispersion.

The phase-matching condition in a crystal can be expressed as follows[11]:

$$\mathbf{k}_\mathrm{i} + \mathbf{k}_\mathrm{a} = \mathbf{k}_\mathrm{d}, \tag{1}$$

where $\mathbf{k}_\mathrm{i}$ and $\mathbf{k}_\mathrm{a}$ are the incident and acoustic wave vectors, respectively, and $\mathbf{k}_\mathrm{d}$ is the diffracted wave vector, as shown in Fig. 1.

In an acoustic-optic crystal, there are two different refraction index surfaces, one for the ordinarily polarized light and the other for the extraordinarily polarized light. In this case, the acoustic wave may diffract incident

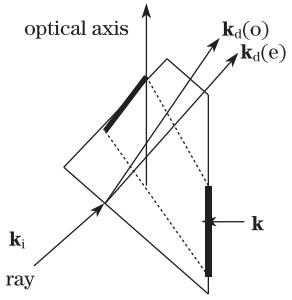

Fig. 1. Geometrical relationship between input wave vector and output wave vector.

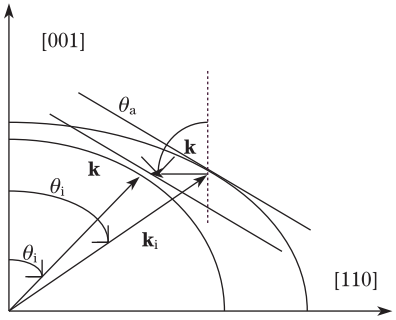

Fig. 2. Diagram of noncollinear AOTF wave vector.

polarized light into orthogonal polarization. For this birefringent diffraction, it is possible to satisfy the phase-matching condition for incident light having a range of incident angles. The acoustic wave vector is chosen so that the tangents to the incident light and the diffracted light wave vector surfaces are parallel, as shown in Fig. 2.

If the acousto-optic crystal rotatory polarization is considered, its right-handed and left-handed elliptical polarized modes have to be treated respectively. On the condition of right-handed elliptical polarized incident beam, the diffracted one is left-handed elliptical polarized mode. The refractive indices of the incident beam and the diffracted beam (n_i, n_d) are as follows:

$$n_\mathrm{i} = \{\cos^2\theta_\mathrm{i}/[n_\mathrm{o}^2(1+\sigma)^2] + \sin^2\theta_\mathrm{i}/n_\mathrm{e}^2\}^{-1/2}, \quad (2)$$

$$n_\mathrm{d} = \{\cos^2\theta_\mathrm{d}/[n_\mathrm{o}^2(1+\sigma)^2] + \sin^2\theta_\mathrm{d}/n_\mathrm{o}^2\}^{-1/2}, \quad (3)$$

where θ_i and θ_d are the polar angles of the incident and the diffracted beams, respectively; n_o and n_e are the ordinary and extraordinary refractive indices in the direction perpendicular to the optical axis, respectively, which are the functions of the optical wavelength λ_0 in vacuum[12]; σ is a parameter related with the rotary, as shown in Fig. 2.

$$n_\mathrm{o} = [1 + 2.5844\lambda_0^2/(\lambda_0^2 - 0.1342^2) + 1.1557\lambda_0^2/(\lambda_0^2 - 0.2638^2)]^{1/2}, \quad (4)$$

$$n_\mathrm{e} = [1 + 2.5825\lambda_0^2/(\lambda_0^2 - 0.1342^2) + 1.5141\lambda_0^2/(\lambda_0^2 - 0.2631^2)]^{1/2}. \quad (5)$$

Equations (2) and (3) can be expressed in elliptical equation forms:

$$y_\mathrm{i}^2/\left[n_\mathrm{o}^2(1+\sigma)^2\right] + x_\mathrm{i}^2/n_\mathrm{e}^2 = 1, \quad (6)$$

$$y_\mathrm{d}^2/\left[n_\mathrm{o}^2(1+\sigma)^2\right] + x_\mathrm{d}^2/n_\mathrm{e}^2 = 1, \quad (7)$$

where y_i and y_d are $\cos\theta_\mathrm{i}/n_\mathrm{i}$ and $\cos\theta_\mathrm{d}/n_\mathrm{d}$, respectively; the derivate of y_i and y_d on the elliptical sphere surfaces of k_i and k_d are $\frac{\mathrm{d}y_\mathrm{i}}{\mathrm{d}x_\mathrm{i}} = -\tan\theta_\mathrm{i} n_\mathrm{o}^2(1+\sigma)^2/n_\mathrm{e}^2$ and $\frac{\mathrm{d}y_\mathrm{d}}{\mathrm{d}x_\mathrm{d}} = -\tan\theta_\mathrm{d}(1-\sigma)^2$, respectively. Considering the momentum-matching condition (Eq. (1)), the following relationship exists:

$$\tan\theta_\mathrm{d} = (n_\mathrm{o}/n_\mathrm{e})^2[(1+\sigma)^2/(1-\sigma)^2]\tan\theta_\mathrm{i}. \quad (8)$$

The polar angle of diffracted beams θ_d is a function of θ_i, n_o, and n_e; θ_d variable extent is asymmetrical compared with θ_i, which causes angular deviation.

Table 1. Parameters Used in Calculation

Parameter	Value				
Rotary (deg./mm)	25.6	86.9	155.95	185	262.8
Wavelength (nm)	1,064	632.8	514.5	488	441.6

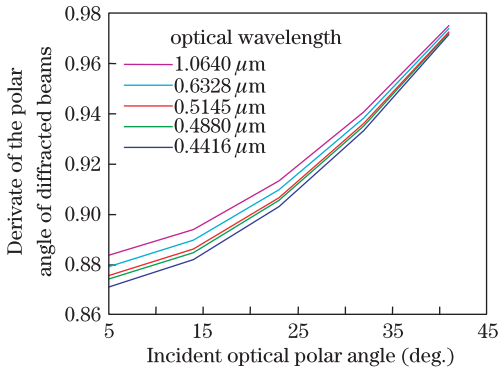

Fig. 3. Variety of polar angles of diffracted beams based on incident optical polar angle.

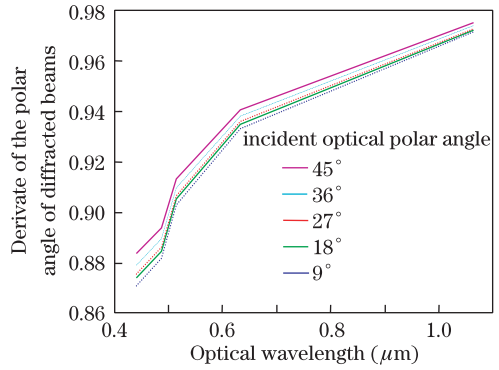

Fig. 4. Variety of polar angles of diffracted beams based on optical wavelength.

The deviation degree can be expressed with the derivate of the polar angle. By using Eq. (8), the derivate of θ_d to θ_i can be determined as follows:

$$\frac{\Delta\theta_\mathrm{d}}{\Delta\theta_\mathrm{i}} = \frac{(n_\mathrm{o}/n_\mathrm{e})^2\left[(1+\sigma)^2/(1-\sigma)^2\right]}{\cos^2\theta_\mathrm{i} + (n_\mathrm{o}/n_\mathrm{e})^4\left[(1+\sigma)^2/(1-\sigma)^2\right]^2\sin^2\theta_\mathrm{i}}. \quad (9)$$

The polar angle of diffracted beams is sensitive to the change in the polar angle of incident beams; Eq. (9) reveals the degree of sensitivity. When the acousto-optic crystal rotatory polarization is considered, the relationships among θ_d, θ_i, n_o, and n_e can be expressed more precisely than that with no consideration of the rotatory polarization in Ref. [11]. According to Eq. (9), where $\mathrm{d}\theta_\mathrm{d}/\mathrm{d}\theta_\mathrm{i}$ to $(n_\mathrm{o}/n_\mathrm{e})^2$ and σ are inversely proportional, the crystal has stronger diffracting power to longer wavelength light and θ_d increases with θ_i. The value of σ can be determined according to the relationship $\sigma = \lambda_0\rho/2\pi n_0$ and the data in Table 1, where ρ is rotary, which has a linear relationship with incident light wavelength. The relationships among $\mathrm{d}\theta_\mathrm{d}/\mathrm{d}\theta_\mathrm{i}$, $(n_\mathrm{o}/n_\mathrm{e})^2$, and σ are exhibited in Figs. 3 and 4.

By considering Snell's law, the relationships among the polar angle of beams and the deviation angle β can be formulated as follows:

$$\sin\beta = n_\mathrm{o}\sin(\theta_\mathrm{i} - \theta_\mathrm{d}). \quad (10)$$

The derivate of the deviation angular can be acquired by the following:

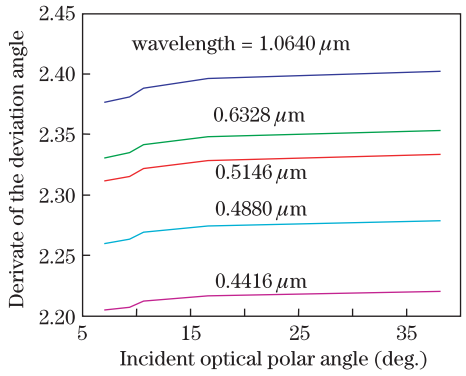

Fig. 5. Deviation angle varies according to incident optical polar angle.

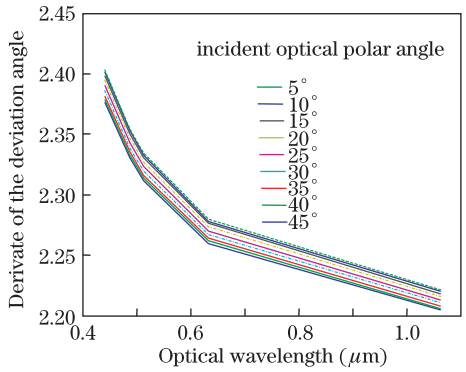

Fig. 6. Deviation angle varies widely according to optical wavelength.

$$\frac{\Delta\beta}{\Delta\theta_{\rm i}} = n_{\rm o}\frac{\cos\{\theta_{\rm i} - \tan^{-1}[A(\lambda_0)\tan\theta_{\rm i}]\}}{\sqrt{1 - n_{\rm o}^2\sin^2\{\theta_{\rm i} - \tan^{-1}[A(\lambda_0)\tan\theta_{\rm i}]\}}} \cdot \left(1 - \frac{\Delta\theta_{\rm d}}{\Delta\theta_{\rm i}}\right), \quad (11)$$

$$A(\lambda_0) = (n_{\rm o}/n_{\rm e})^2\,[(1+\sigma)^2/(1-\sigma)^2]. \quad (12)$$

According to Eq. (11), the degree of β deviation is a function of $\theta_{\rm i}$ and λ_0. The deviation of β decreases with the wavelength of incident beams when the beams are at a fixed optical polar angle, as shown in Fig. 5. And the deviation increases distinctively with incident optical polar angle when incident beams are at a certain wavelength within 0.4–1.0 μm, shown in Fig. 6.

In practical applications, parallel incident optical beams cannot propagate perpendicularly with the input facet into crystal without any error because of the manufacturing aspect or other reasons; the small deviation of incident optical polar angle is difficult to be avoided. When the wavelength of the incident optical beams is 0.6328 μm, $\theta_{\rm i}$ is 25, and β deviation is 2.34 times of $\theta_{\rm i}$. In the design of AOTF, another wedge angle should be applied to its output facet to conquer scene shift caused by $\theta_{\rm i}$ dispersion; $\Delta\beta/\Delta\theta_{\rm i}$ is in the 2.2–2.4 range, thus we can adopt $\Delta\beta/\Delta\theta_{\rm i} = 2.3$ to design the wedge angle.

In conclusion, we have given an analysis of the deviation of diffracted beams caused by crystal diffraction in AOTF multispectral imaging systems considering the rotatory property with birefringence. The rotatory property has a significant influence on the design of the AOTF, especially in conquering scene shift. It is proven that another wedge should be added to the output facet. Our analysis is meaningful in improving the performance of AOTF.

This work was supported by the National "973" Project of China under Grant No. 2007CB310606.

References

1. H. Kao, H. Ren, and C. Lee, J. Appl. Remote Sens. **2,** 023536 (2008).
2. L. Zhao and S. Walfik, Focus Molec. Imag. **10,** 1563 (2009).
3. J. Svensson, J. Axelsson, A. Johansson, N. Bendsoe, K. Svanberg, and S. Andersson **1-2,** 227 (2006).
4. P. E. Geissler, R. Greenberg, G. Hoppa, A. Mcewen, R. Tufts, and C. Phillios, Icarus **135,** 107 (1998).
5. B. Liu, W. Liu, and J. Peng, Chin. Opt. Lett. **8,** 384 (2010).
6. Y. Hiraoka, T. Shimi, and T. Haraguchi, Cell Struct. Funct. **27,** 367 (2002).
7. F. Moreau, S. M. Moreau, D. M. Hueber, and T. Vo-Dinh, Appl. Spectrosc. **50,** 1295 (1996).
8. I. C. Chang, Opt. Eng. **20,** 824 (1981).
9. Y. Yano and A. Watanabe, Appl. Opt. **15,** 2250 (1976).
10. D. A. Glenar, J. J. Himan, B. Saif, and J. Bergstrahl, Appl. Opt. **33,** 7412 (1994).
11. I. C. Chang, Appl. Phys. Lett. **25,** 370 (1974).
12. N. Uchida, Phys. Rev. B **4,** 3736 (1971).